# Proton scattering at RIA and microscopic optical potentials.

*S. Karataglidis*

*LANL*

# Introduction

We define the Nucleon-Nucleus ($NA$) optical potential in terms of an effective potential based on the $g$ matrices for infinite nuclear matter obtained from the Bruckner-Bethe-Goldstone equation:

$$g_{LL'}^{(JST)}(p',p;k,k_f) = V_{LL'}^{(JST)}(p',p) + \frac{2}{\pi}\sum_l \int_0^\infty V_{Ll}^{(JST)}(p',q)\,[\mathcal{H}]\,g_{lL'}^{(JST)}(q,p;k,k_f)\,q^2\,dq$$

where $V_{LL'}^{(JST)}(p',p)$ is the $NN$ interaction and

$$\mathcal{H}(q,k,K,k_f) = \frac{\bar{Q}(q,K;k_f)}{\bar{E}(q,K;k_f) - \bar{E}(k,K;k_f) - i\varepsilon}.$$

Thus, the $NA$ optical potential is defined for all spin ($S$) and isospin ($T$) channels. We should then be able to use the same microscopic optical potential to describe both proton-nucleus and neutron-nucleus scattering observables.

The optical potential itself is (as defined in coordinate space):

$$U\left(\mathbf{r}_1,\mathbf{r}_2;E\right)=\sum_n \zeta_n\left\{\delta\left(\mathbf{r}_1-\mathbf{r}_2\right)\int \varphi_n^*(\mathbf{s})v_D(\mathbf{r}_{1s})\varphi_n(\mathbf{s})\,d\mathbf{s}\right.$$
$$\left.+\,\varphi_n^*(\mathbf{r}_1)v_{Ex}(\mathbf{r}_{12})\varphi_n(\mathbf{r}_2)\right\}$$
$$\Rightarrow U_D(\mathbf{r}_1;E)+U_{Ex}(\mathbf{r}_1,\mathbf{r}_2;E)$$

where the $\zeta_n$ are the one-body density matrix elements of the target ground state. We can thus predict observables for $NA$ scattering with a reasonable model of structure. Hence the shell model may be used to predict scattering observables of interest when there may be no data available.

We make comparisons between $pA$ and $nA$ scattering observables for the same target to test the initial conjecture: that the same OMP may be used for both. Examples: $^{12}$C, $^{28}$Si, and $^{90}$Zr, at 65 MeV.

## Example: $^{12}$C

Model used: $(0+2)\hbar\omega$ shell model using the WBT interaction of Warburton and Brown. HO wave functions chosen to reproduce electron scattering data.

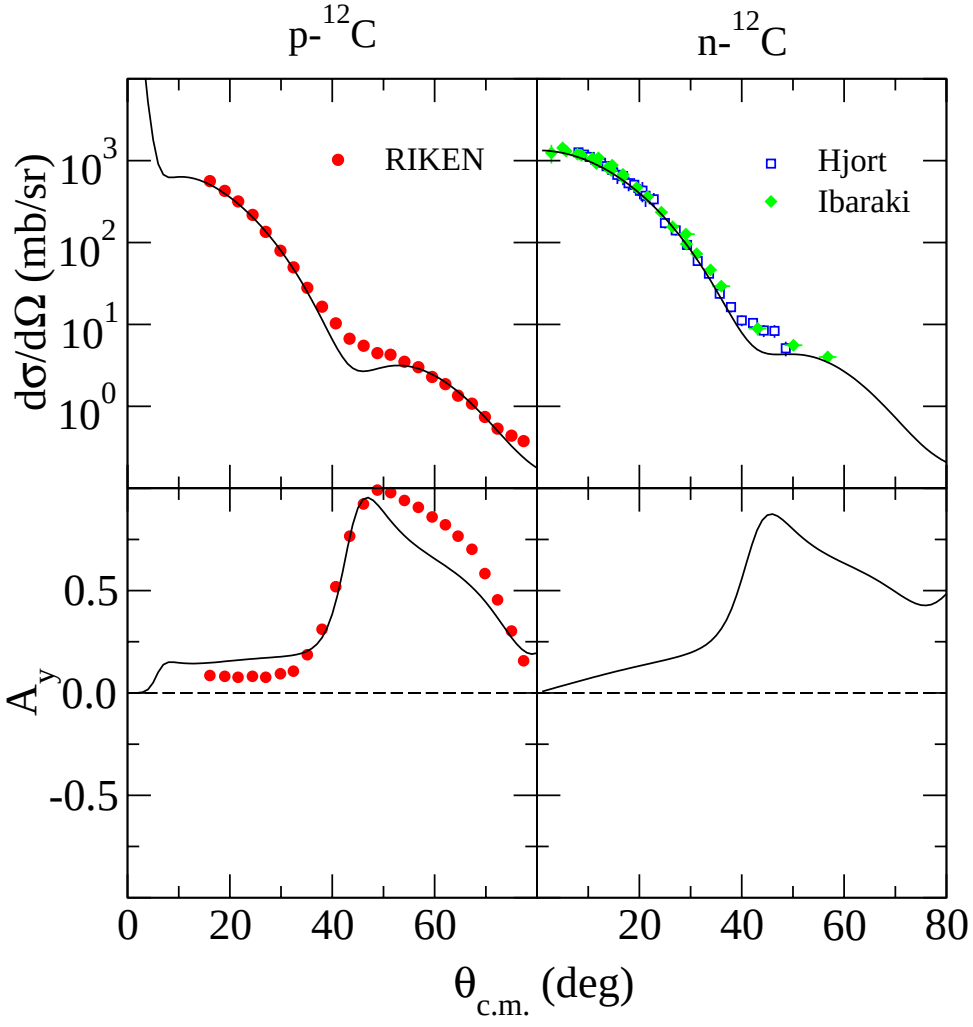


Figure 1: $N$-$^{12}$C scattering observables at 65 MeV.

Intergrated cross sections:

Proton reaction cross section: $\sigma_R = 324.35$ mb (theory), $= 310 \pm 13$ mb (experiment, 60.8 MeV).

Neutron cross sections:

| | MOMP | Evaluation (WS model) |
|---|---|---|
| $\sigma_{el}$ (mb) | 471.11 | 463.45 |
| $\sigma_R$ (mb) | 330.96 | 291.93 |
| $\sigma_{tot}$ (mb) | 748.07 | 755.38 |

The total cross sections are equivalent. Hence the higher reaction cross section predicted by the microscopic model, and subsequent lower elastc scattering cross section, would suggest that the microscopic OMP has a stronger imaginary part, and weaker real part, than the phenomenological OMP used in the evaluation of the data.

## $^{28}$Si

Model used: $sd$-shell model with USD interaction. HO wave functions chosen to reproduce rms radius.

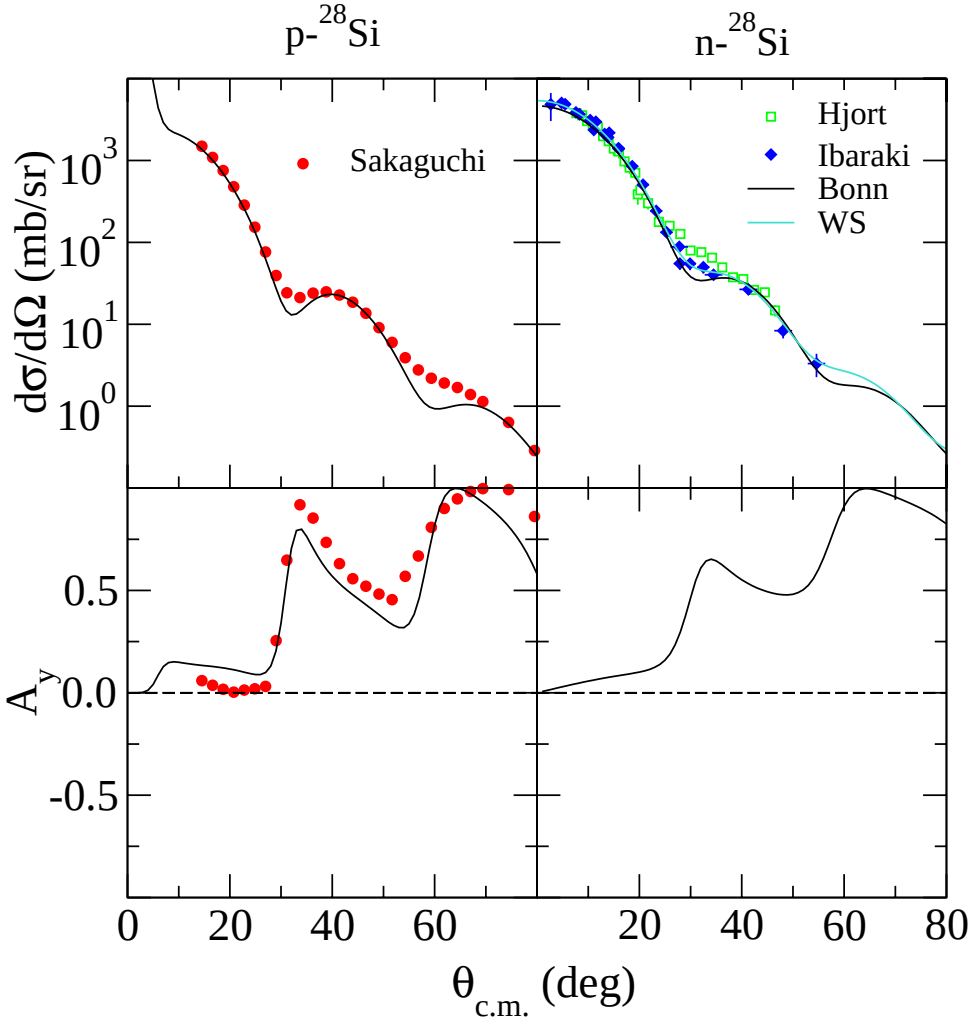


Figure 2: $N$-$^{28}$Si scattering observables at 65 MeV.

Integrated cross sections:

Proton reaction cross section: $\sigma_R = 596.75$ mb (theory). (No data available at this energy.)

Neutron cross sections:

| | MOMP | Evaluation (WS model) |
|---|---|---|
| $\sigma_{el}$ (b) | 0.598 | 0.522 |
| $\sigma_R$ (b) | 0.852 | 0.996 |
| $\sigma_{tot}$ (b) | 1.450 | 1.518 |

As with $^{12}$C, one sees a greater reaction cross section at the expense of the elastic. That is consistent with there being a stronger imaginary part of the potential. The lower overall total cross section in the MOMP indicates a problem describing the surface details in the structure.

## $^{90}$Zr

Model used: nis-shell model ($0f_{5/2}$, $1p_{3/2}$, $1p_{1/2}$, $0g_{9/2}$) with nisj interaction of Ji and Wildenthal. HO wave functions chosen to reproduce rms radius.

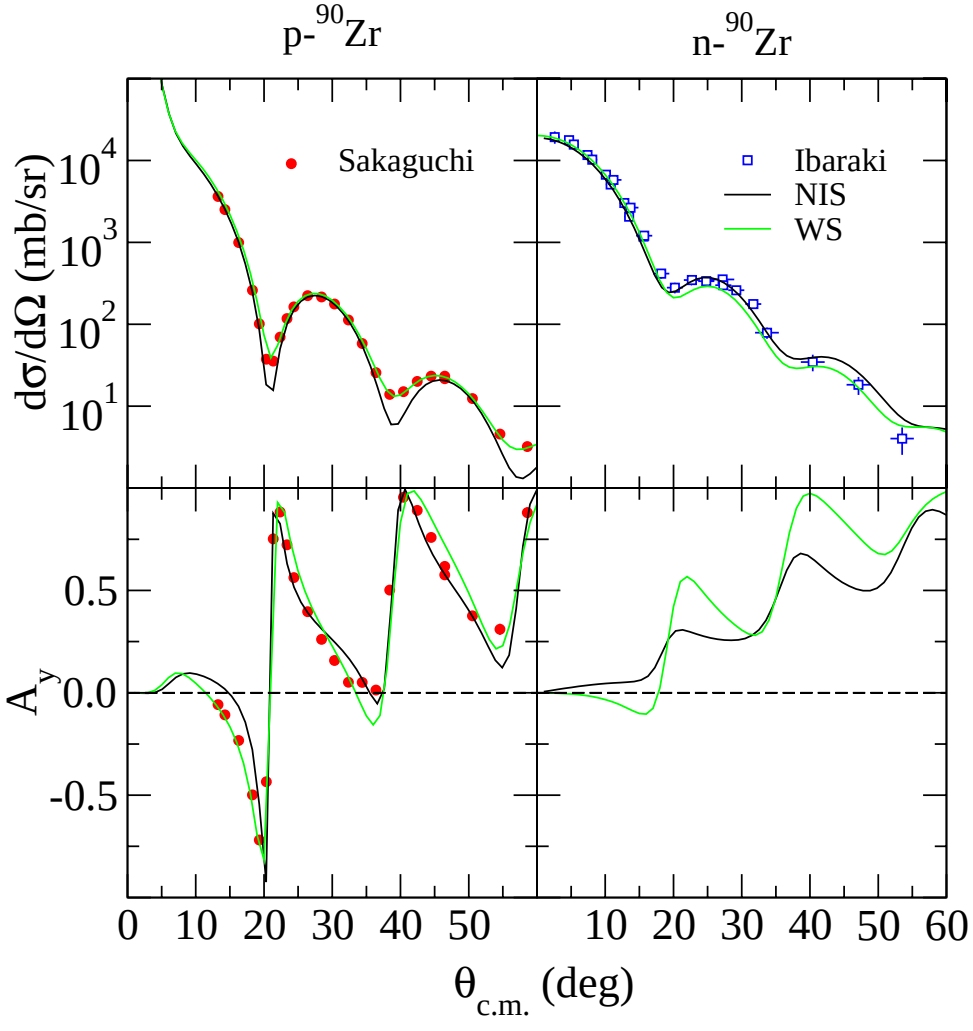


Figure 3: $N$-$^{90}$Zr scattering observables at 65 MeV.

Integrated cross sections:

Proton reaction cross section: $\sigma_R = 1.259$ b (theory). $= 1.144 \pm 0.042$ b (experiment, 60.8 MeV). Neutron cross sections:

| | MOMP |
|---|---|
| $\sigma_{el}$ (b) | 1.299 |
| $\sigma_R$ (b) | 1.714 |
| $\sigma_{tot}$ (b) | 3.013 |

(No evaluation of data was done of these observables at this energy.)

**Application to actinides** As ATW will require lower energies, the energy dependence for neutron scattering from $^{238}$U is presented.

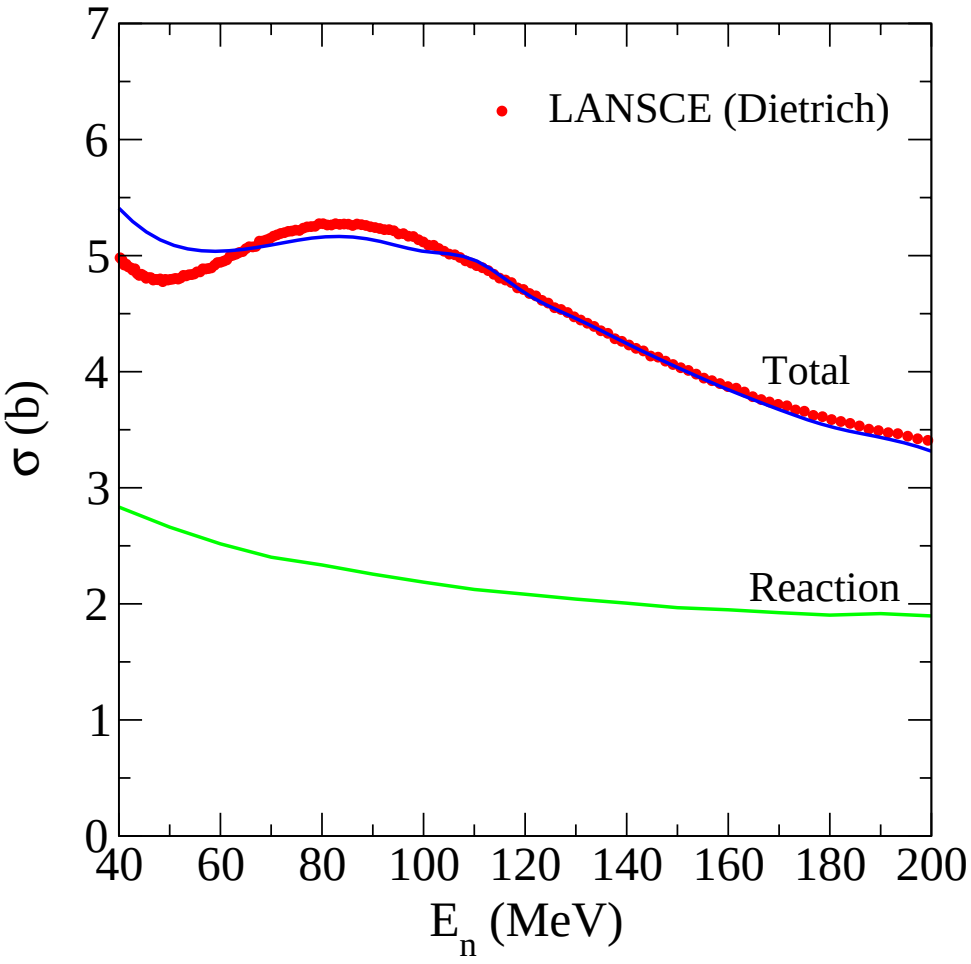


Figure 4: Total and reaction cross section for $n$-$^{238}$U scattering.

As one proceeds to lower energies, the agreement with experiment worsens.

# Conclusions

- The same microscopic optical potentials which have worked in the past for $pA$ scattering work equally well for $nA$ scattering.
- The additional quantities obtainable for $nA$ scattering are also well described using the same optical potentials.
- The analysis gives support to the use of the shell model to predict neutron-nucleus scattering observables in the cases where there are no data, without the need to use any parametric form of the optical potentials involved.
- An extension of the model is required to lower energies in order to predict the cross sections needed for ATW. RIA will allow the testing of the optical potentials in those cases that can be measured.